JVST A
Journal of Vacuum Science & Technology A

Characterization of plasma-enhanced atomic layer deposition of Al_2O_3 using dimethylaluminum isopropoxide

Cite as: J. Vac. Sci. Technol. A **32**, 021514 (2014); https://doi.org/10.1116/1.4866378
Submitted: 04 December 2013 • Accepted: 10 February 2014 • Published Online: 25 February 2014

Jialing Yang, Brianna S. Eller, Manpuneet Kaur, et al.

Characterization of plasma-enhanced atomic layer deposition of Al_2O_3 using dimethylaluminum isopropoxide

Jialing Yang and Brianna S. Eller
Department of Physics, Arizona State University, Tempe, Arizona 85287-1504

Manpuneet Kaur
School for Engineering of Matter, Transport and Energy, Arizona State University, Tempe, Arizona 85287-6106

Robert J. Nemanich[a)]
Department of Physics, Arizona State University, Tempe, Arizona 85287-1504

(Received 4 December 2013; accepted 10 February 2014; published 25 February 2014)

In this research, Al_2O_3 films were grown by remote plasma-enhanced atomic layer deposition using a nonpyrophoric precursor, dimethylaluminum isopropoxide (DMAI), and oxygen plasma. After optimization, the growth rate was determined to be ~1.5 Å/cycle within a growth window of 25–220 °C; the higher growth rate than reported for thermal atomic layer deposition was ascribed to the higher reactivity of the plasma species compared with H_2O and the adsorption of active oxygen at the surface, which was residual from the oxygen plasma exposure. Both effects enhance DMAI chemisorption and increase the saturation density. In addition, a longer oxygen plasma time was required at room temperature to complete the reaction and decrease the carbon contamination below the detection limit of x-ray photoemission spectroscopy. The properties of the subsequent Al_2O_3 films were measured for different temperatures. When deposited at 25 °C and 200 °C, the Al_2O_3 films demonstrated a single Al-O bonding state as measured by x-ray photoemission spectroscopy, a similar band gap of 6.8±0.2 eV as determined by energy loss spectroscopy, a similar index of refraction of 1.62±0.02 as determined by spectroscopic ellipsometry, and uniform growth with a similar surface roughness before and after growth as confirmed by atomic force microscopy. However, the room temperature deposited Al_2O_3 films had a lower mass density (2.7 g/cm^3 compared with 3.0 g/cm^3) and a higher atomic ratio of O to Al (2.1 compared with 1.6) as indicated by x-ray reflectivity and Rutherford backscattering spectroscopy, respectively. © *2014 American Vacuum Society*. [http://dx.doi.org/10.1116/1.4866378]

I. INTRODUCTION

Thin films of Al_2O_3 have been used as dielectric layers for Si and III-V microelectronics.[1–5] The potential of Al_2O_3 for this application is linked to advantageous dielectric properties such as a large band gap (~6.5 eV),[6,7] relatively high dielectric constant (~8),[1,8] high breakdown field (~10 MV/cm), chemical and thermal stability, and adhesion to many surfaces. In addition to metal-oxide-semiconductor structures, Al_2O_3 has also been considered for a range of applications, including corrosion protection on metallic substrates,[9,10] passivation of solar cells,[11,12] coatings of optical devices,[13,14] and diffusion barriers in organic electronics.[15,16] Given the significant potential and range of applications associated with Al_2O_3, there has been considerable effort during the last several decades to establish and develop methods for Al_2O_3 deposition, including chemical vapor deposition (CVD),[17] physical vapor deposition,[15] and, one of the most promising, atomic layer deposition (ALD). ALD has often been preferred as an advanced thin film deposition technique due to the high-quality films obtained. More specifically, ALD films have been achieved at low temperatures with low impurity content and uniform and conformal coverage.[18,19]

ALD is based on the sequential use of gas phase chemical processes;[1,18] assuming a binary reaction mechanism, there are two precursors that interact with the surface independently as they are separated by purge steps. Consequently, this process results in flux-independent, self-limiting, layer-by-layer deposition with precise atomic-scale thickness control of conformal and uniform films on large diameter and/or high aspect ratio substrates.[18,20] Explicitly, this ALD process includes the following four steps: first, a self-limiting reaction between the surface −OH groups and precursor; second, a purge step to remove nonreacted precursor and gaseous by-products; third, a self-limiting reaction between a H_2O reactant and the surface groups; and lastly, a second purge step, resulting in a fresh starting surface for subsequent cycles.

For ALD of Al_2O_3, the binary reaction between trimethylaluminum (TMA, $Al(CH_3)_3$) and H_2O in thermal ALD remains one of the most extensively studied[1,18]

$$\begin{aligned} &\|-OH_{(ads)} + Al(CH_3)_{3(g)} \rightarrow \|-OAl(CH_3)_{2(ads)} + CH_{4(g)} \\ &\|-AlCH_{3(ads)} + H_2O_{(g)} \rightarrow \|-Al(OH)_{(ads)} + CH_{4(g)}. \end{aligned} \quad (1)$$

In these equations, "‖−" represents surface bound species, "ads" chemisorbed molecules, and "g" gas phase chemicals and by-products. This is an advantageous process as the

a)Electronic mail: robert.nemanich@asu.edu

reactivity results in self-limiting behavior. Furthermore, TMA is thermally stable with a high vapor pressure at room temperature [9 Torr at 16.8 °C (Ref. 21)], leading to reliable chemisorption, and the by-products of the reaction (e.g., CH_4) do not interfere with the deposition or purity of the film.

Despite the extensive use of TMA-based ALD processes, the safety of TMA remains a concern; it is not only pyrophoric but also highly reactive with H_2O. Reports from Eindhoven University of Technology have presented a detailed study of ALD Al_2O_3 using TMA (Refs. 22–25) and alternative nonpyrophoric precursor, dimethylaluminum isopropoxide (DMAI, $[(CH_3)_2AlOCH(CH_3)_2]_2$).[21]

The properties of TMA and DMAI have been reported.[21] DMAI has a vapor pressure appropriate for ALD processes, it is not pyrophoric, and it is more stable than TMA. Unlike TMA, DMAI is not a symmetric molecule. Thus, there are several surface reactions that may occur during ALD; the most likely have been reported as

$$\begin{aligned} &||-OH_{(ads)} + \frac{1}{2}\left[(CH_3)_2AlOCH(CH_3)_2\right]_{2(g)} \\ &\quad \rightarrow ||-OAl(CH_3)OCH(CH_3)_{2(ads)} + CH_{4(g)} \\ &||-AlOCH(CH_3)_{2(ads)} + H_2O_{(g)} \rightarrow ||-Al(OH)_{(ads)} \\ &\quad + HOCH(CH_3)_{2(g)}, \end{aligned} \tag{2}$$

and/or

$$\begin{aligned} &||-OH_{(ads)} + \frac{1}{2}\left[(CH_3)_2AlOCH(CH_3)_2\right]_{2(g)} \\ &\quad \rightarrow ||-OAl(CH_3)_{2(ads)} + HOCH(CH_3)_{2(g)} \\ &||-Al(CH_3)_{(ads)} + H_2O_{(g)} \rightarrow ||-Al(OH)_{(ads)} + CH_{4(g)}. \end{aligned} \tag{3}$$

Evidence suggests that these different surface reactions [e.g., Eqs. (2) and (3)] occur simultaneously.[21]

In addition to altering the precursor, researchers at Eindhoven University of Technology have also evaluated the effects of various oxidizers. The study was completed using both TMA and DMAI to deposit Al_2O_3 in plasma enhanced atomic layer deposition (PEALD). PEALD is an energy enhanced ALD method[3,19] that uses an activated plasma species (e.g., O_2* and O*) as the oxidizer rather than H_2O. The plasma process offers advantages over the thermal process, where the reactivity of the oxygen species results in not only an increased growth rate and film density but also a decreased impurity concentration and growth temperature.[26,27] Consequently, PEALD with O_2 plasma allows for a wider range of substrates that may require a low temperature deposition process, such as plastic based flexible displays and polymers,[28,29] as well as more stable precursors that may not be reactive with H_2O.[19] Additionally, O_2 is more readily purged than H_2O, which improves the growth efficiency and reduces cycle time. PEALD also enables better control of film composition than thermal ALD as the technique permits the admixing of gases into the plasma[19,26] or adjusting other parameters such as plasma power and working pressure.[19,30,31]

For plasma-enhanced atomic layer deposition, Langereis *et al.*[23] and Potts *et al.*[21] identified the following reactions using TMA as:

$$\begin{aligned} &||-OH_{(ads)} + Al(CH_3)_{3(g)} \rightarrow ||-OAl(CH_3)_{2(ads)} + CH_{4(g)} \\ &||-AlCH_{3(ads)} + 4\,O^*_{(g)} \rightarrow ||-Al(OH)_{(ads)} + H_2O_{(g)} \\ &\quad + CO_{2(g)}, \end{aligned} \tag{4}$$

and DMAI as

$$\begin{aligned} &||-OH_{(ads)} + \frac{1}{2}\left[(CH_3)_2AlOCH(CH_3)_2\right]_{2(g)} \\ &\quad \rightarrow ||-OAl(CH_3)OCH(CH_3)_{2(ads)} + CH_{4(g)} \\ &||-AlOCH(CH_3)_{2(ads)} + 9\,O^*_{(g)} \rightarrow ||-Al(OH)_{(ads)} \\ &\quad + 3CO_{2(g)} + 3\,H_2O_{(g)}, \end{aligned} \tag{5}$$

and/or

$$\begin{aligned} &||-OH_{(ads)} + \frac{1}{2}\left[(CH_3)_2AlOCH(CH_3)_2\right]_{2(g)} \\ &\quad \rightarrow ||-OAl(CH_3)_{2(ads)} + HOCH(CH_3)_{2(g)} \\ &||-Al(CH_3)_{(ads)} + 4\,O^*_{(g)} \rightarrow ||-Al(OH)_{(ads)} \\ &\quad + CO_{2(g)} + H_2O_{(g)}, \end{aligned} \tag{6}$$

where these two binary reactions [e.g., Eqs. (5) and (6)] are likely to occur simultaneously.[21] This indicates that the surface is presumable terminated by −OH groups after O_2 plasma exposure.

While plasma-enhanced ALD processes have the potential to alter the chemical reactions and the surface reaction mechanisms, there are a range of results that appear inconsistent. For instance, thermal ALD with DMAI has a reported Al_2O_3 growth rate that is greater than that for PEALD with DMAI.[21] More significantly, the growth rate of Al_2O_3 using PEALD and DMAI (~0.9–1.2 Å/cycle) has been reported to be lower than PEALD using TMA (1.4 Å/cycle).[21,32] X-ray photoemission spectroscopy (XPS) studies of the different films have shown multiple O bonding configurations and in some cases multiple Al bonding configurations.[21] The same studies have shown differences in the residual carbon concentrations.

Even with the extensive prior studies, there is still disagreement or apparently conflicting results on (1) the PEALD growth rate using DMAI; (2) the bonding configurations of the deposited Al atoms; and (3) the presence of carbon impurities. These uncertainties may have limited the acceptance of DMAI for ALD applications.

In this research, the uncertainties noted above have been addressed through a detailed study of PEALD-DMAI Al_2O_3 film deposition with a specific focus on the O_2 plasma conditions, which has not been extensively reported to date. In addition, this study includes results on film morphology and

band gap measurement to better characterize the films. Our results establish that the growth rate of the PEALD DMAI process could be equivalent to the PEALD TMA process; the growth rate of the plasma process could be higher than the thermal process; the films exhibit predominantly a single Al bonding configuration; the carbon contamination could be reduced to the XPS detection limit; the film morphology reflected the substrate roughness; and the band gap was comparable to the ALD Al_2O_3 using TMA.

II. EXPERIMENT

Al_2O_3 films were deposited by remote PEALD using DMAI and O_2 plasma on oxidized n-type Si (100) substrates. The PEALD Al_2O_3 was completed in a custom system shown schematically in Fig. 1.[3,33] The system base pressure was $\sim 6.0\times10^{-9}$ Torr, and during deposition, the pressure increased to $\sim$100 mTorr as controlled by a throttle valve in front of the turbo pump. The DMAI precursor was heated to 90 °C in the bubbler to provide sufficient vapor pressure and was delivered to the chamber with an Ar carrier gas at a flow rate of 90 standard cubic centimeters per minute (sccm). To prevent condensation during precursor exposure, the chamber and delivery lines were maintained at $\sim$110 °C. Research grade N_2 with a flow rate of 35 sccm was used as the purge gas, and ultrahigh purity grade O_2 with a flow rate of 35 sccm was used as the oxidizer. A 6 s O_2 purge preceded exciting the plasma. The remote plasma was generated by an inductively coupled rf-source (200 W and 13.56 MHz) $\sim$25 cm above the sample, which reduces the ion concentration while providing a sufficient flux of excited molecular species and radicals.

The timing of the gas pulses and plasma power were first varied to ensure saturated adsorption and self-limiting growth for a substrate temperature expected to be within the growth window. The ALD growth window was then determined, where the substrate temperature was varied between 25 °C and 350 °C (measured using a thermocouple and infrared pyrometer). For room temperature growth, both the substrate and chamber temperature were reduced to room temperature, but the bubbler and delivery line were maintained at 90 and 110 °C to provide consistent vapor pressure and prevent precursor condensation. However, even with the elevated precursor temperature, the thermocouple near the sample consistently indicated room temperature during deposition.

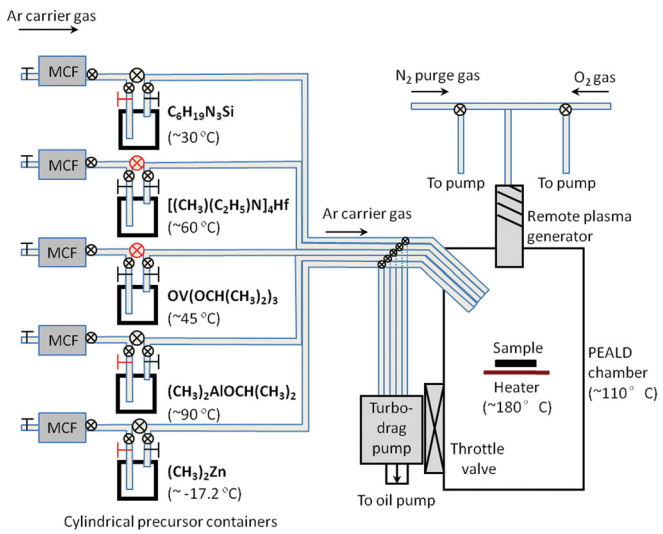

FIG. 1. (Color online) Schematic of the remote plasma-enhanced atomic layer deposition chamber.

Film thicknesses were determined with an *in-situ* quartz crystal microbalance (QCM) and XPS core level intensities and corroborated by comparison with *ex-situ* x-ray reflectivity (XRR), Rutherford backscattering spectroscopy (RBS), and spectroscopic ellipsometry (SE). The chemical states and composition of the films were then analyzed using *in-situ* XPS and ultraviolet photoemission spectroscopy (UPS).[3,34] Other material properties such as thin film density, surface morphology, index of refraction, and band gap energy were determined from XRR, AFM, SE, and energy loss spectroscopy (ELS), respectively.

III. RESULTS AND DISCUSSION

A. PEALD Al_2O_3 growth

1. Self-limiting growth

To ensure uniform and conformal ALD growth, each half-reaction must be fully saturated and self-limiting within the ALD growth window; therefore, PEALD of Al_2O_3 using DMAI was first optimized with regards to the timing of the reactants and purge gases for a substrate temperature of 200 °C, which was within the reported growth window.[21,32]

As shown in Fig. 2(a), the growth rate of Al_2O_3 at 200 °C reached self-limiting behavior when the DMAI precursor pulse was $\geq$0.2 s, the O_2 plasma was generated for $\geq$6 s, and the N_2 purge time was $\geq$18 s. Therefore, a 0.6 s DMAI precursor pulse and 8 s O_2 plasma exposure were employed for other processes at 200 °C. This timing ensured DMAI chemisorption was saturated, and O_2 plasma reacted fully with the adsorbed species at this temperature. A longer N_2 pulse time (20 s) was chosen to ensure ample purge time, thus limiting CVD-like reactions between the reactants and removing gas-phase by-products from the chamber. The relationship between the growth rate and O_2 plasma power was also investigated in this study as shown in Fig. 2(b). The results indicated that the growth rate increased with plasma power between 30 and 150 W and stabilized for power >150 W. Consequently, a plasma power of 200 W was adopted for subsequent growth conditions.

Film thicknesses, and thus the growth per cycle (GPC), were determined *in-situ* by QCM and XPS core level intensities. These measurements were then corroborated with XRR, RBS, and SE of thicker Al_2O_3 films (>25 nm) grown under the same conditions. Figure 3 shows the XRR data for 200 cycles Al_2O_3 deposited at 200 °C, indicating a film thickness of 30.4 nm. These results thus imply a GPC of $\sim$1.5 Å/cycle.

This growth rate is higher than the growth rates measured by other groups using DMAI for thermal ALD, $\sim$0.7–1.2 Å/cycle at temperatures $\sim$150–200 °C.[21,35] The

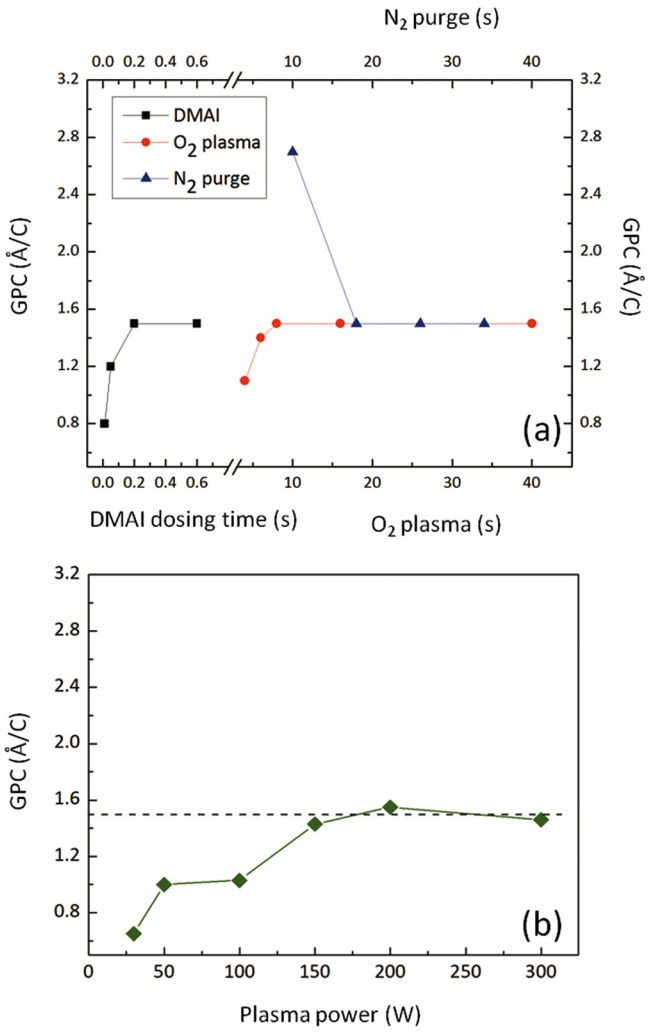

FIG. 2. (Color online) Al_2O_3 growth rate vs (a) DMAI dose time (squares), N_2 purge time (triangles), and O_2 plasma exposure time (circles); (b) vs plasma power (diamonds) at a substrate temperature of 200 °C.

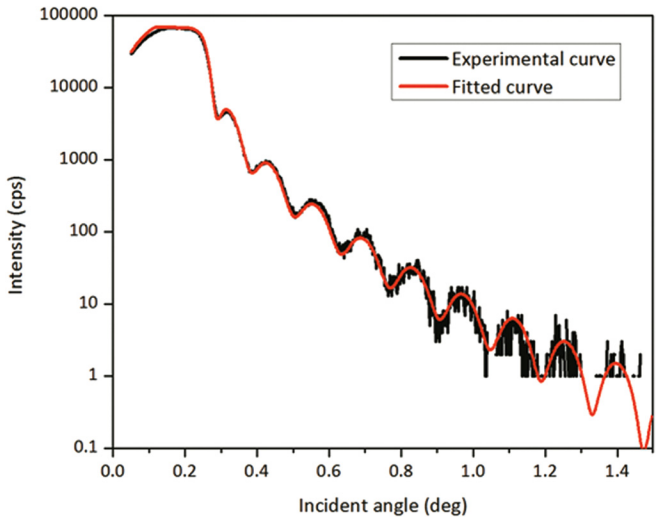

FIG. 3. (Color online) XRR of ~30 nm Al_2O_3 film deposited with optimized growth parameters on Si. The line with noise refers to the measured data, and the smooth line refers to the fitted results.

larger growth rate associated with PEALD has been previously documented and related to the higher reactivity of the oxygen species compared with H_2O and active oxygen groups remaining on the surface after the plasma step.[21,24,26,36] There are three mechanisms that could account for the increased growth rate:[21,26,36] an increase in the reactivity of the oxygen species, an increase in the density of surface reactive sites, and/or a reduction of steric hindrance, where the ligands of the DMAI monomer or dimer (e.g., isopropoxide group) overlap with available reactive sites and prevent chemisorptions.[21,37,38] The increased reactivity represents an increase in the kinetics of the process, while the other effects increase the available absorption sites. The excess active oxygen groups, perhaps −OH groups, could serve as additional reactive sites and thus increase the density of chemisorbed DMAI molecules. In addition, the active oxygen species could react with ligands from depositing precursor molecules, thus reducing steric hindrance and exposing additional reactive sites for chemisorption or generating additional surface sites. Consequently, the active oxygen plasma species could accelerate the surface reactions, increase the surface density of −OH sites, and/or reduce steric hindrance through reactions with precursor ligands. This hypothesis may also explain the relationship between the growth rate and O_2 plasma power, where the increase in plasma power increases the concentration of activated oxygen species and thus the growth rate. Under the experimental conditions, the PEALD growth rate using DMAI was improved by 30–80% compared with some prior studies[21,32] and is then comparable with PEALD using a TMA process (1.4 Å/cycle).[32]

One of the concerns about the enhanced growth rate of PEALD is that it could result in nonuniform growth. AFM was thus used to determine the morphology of the surfaces before and after growth of 6 nm and 33 nm thick PEALD Al_2O_3 films grown at 200 °C and 25 °C, respectively. These results are shown in Fig. 4. The RMS roughness was ~0.77±0.05 nm for the cleaned Si wafer [Fig. 4(a)], 0.76±0.05 nm for Al_2O_3 films grown at 200 °C [Fig. 4(b)], and 0.86±0.05 nm for Al_2O_3 films deposited at 25 °C [Fig. 4(c)]. These results indicated uniform and conformal deposition of Al_2O_3 films, where neither the O_2 plasma nor the increased growth rate resulted in increased surface roughness.

2. PEALD growth window

To further explore the growth properties at different conditions, the number of Al atoms deposited per cycle at different growth temperatures was determined by RBS, and the results are shown in Fig. 5(a). The Al atoms deposited per cycle increased with temperature above 200 °C, and decreased when the temperature was reduced below 100 °C. Within the temperature range of 150–200 °C, the Al atoms deposited per cycle was similar.

The substrate temperature growth window was also investigated. As shown in Fig. 6, these growth conditions resulted in a PEALD temperature window of ~25–220 °C. Within the temperature window, the growth is self-limiting with a constant growth rate, as shown by the linear relationship

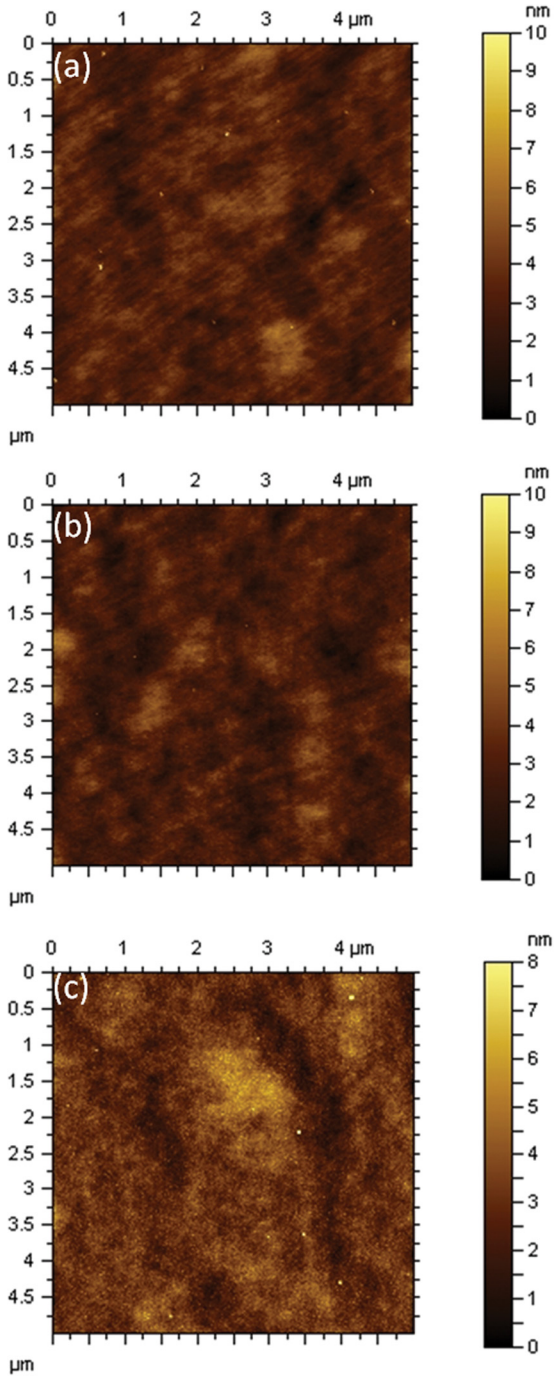

FIG. 4. (Color online) AFM images of (a) degreased Si wafer, (b) as-grown 6 nm Al_2O_3 film deposited at 200 °C, and (c) as-grown 33 nm Al_2O_3 film deposited at 25 °C. Images are 5 μm × 5 μm. The RMS roughnesses were ~0.77±0.05, 0.76±0.05, and 0.86±0.05 nm, respectively.

between the film thickness and number of PEALD cycles at 200 °C. At temperatures >220 °C, the growth rate increased with substrate temperature, suggesting DMAI thermally decomposed on the surface. In contrast, at room temperature, the growth rate was slightly reduced, suggesting an incomplete reaction. In this case, an incomplete reaction could refer to when DMAI molecules were not effectively bonded to the surface groups and thus purged out of the chamber, and/or the O_2 plasma did not complete the oxidation reaction as a result of insufficient thermal energy.

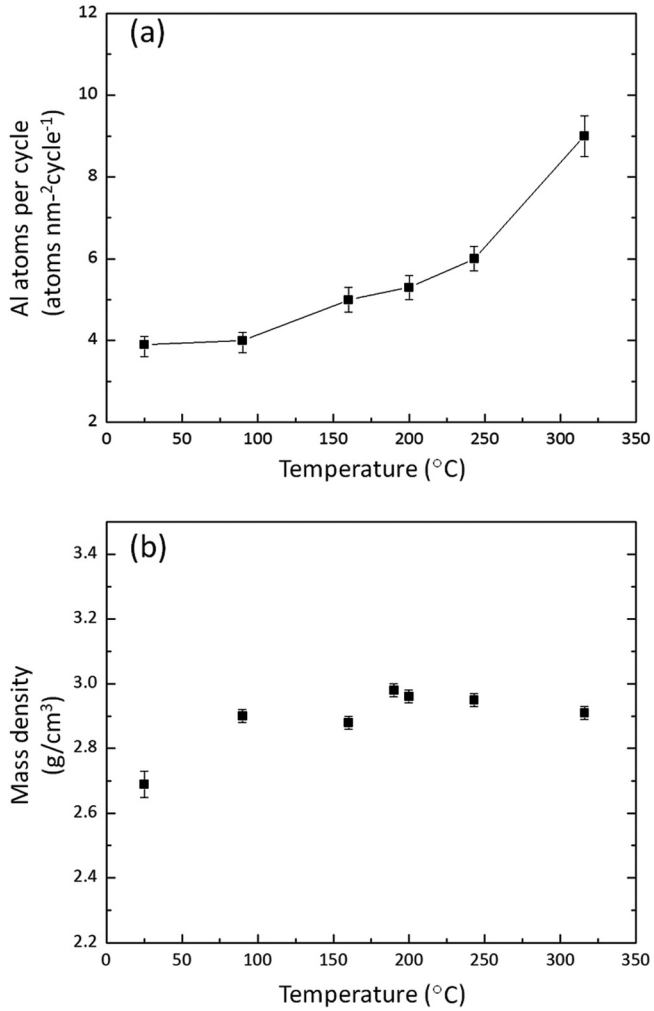

FIG. 5. Number of Al atoms deposited per cycle (a) as determined by RBS and the film mass density, and (b) as measured by XRR for PEALD Al_2O_3 film using DMAI at different temperatures.

For the room temperature growth, if the DMAI chemisorption was not complete, then increasing the DMAI pulse time may lead to an increased growth rate. Conversely, if the incomplete reactions were limited by the oxidation process, then increasing the oxygen plasma exposure could lead to an increased growth rate. To investigate this point, Al_2O_3 films were grown with an increased DMAI dosing time of 1.2 s and N_2 purge time of 30–50 s to prevent CVD-like reactions. These deposition parameters again resulted in a growth rate of ~1.4 Å/cycle at room temperature, which suggested the longer DMAI dose time did not increase the DMAI chemisorption at this temperature. (The growth rate of Al_2O_3 at 200 °C under these same conditions remained at 1.5 Å/cycle, further confirming saturation at 200 °C.) On the other hand, increasing the O_2 plasma exposure from 8 to 40 s increased the 25 °C Al_2O_3 growth rate by ~10% to ~1.5 Å/cycle. This suggested that a longer oxygen plasma time is required to drive the chemical reaction at the lower temperature.

Comparing the Al_2O_3 films deposited at 25 °C and 200 °C, even though the concentration of Al atoms per cycle deposited at 25 °C was 26% smaller than that at 200 °C (3.9±0.2 at. nm^{-2}cycle^{-1} compared with 5.3±0.3 at.

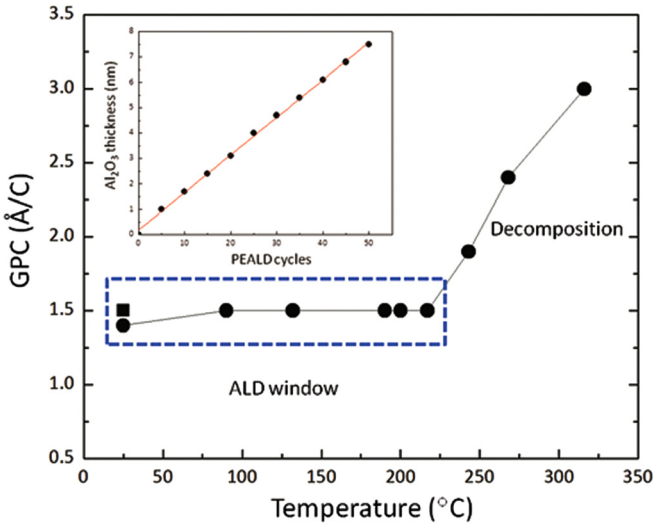

FIG. 6. (Color online) Al_2O_3 growth rate vs substrate temperature, determining the ALD window of 25 °C–220 °C. The square represents the increased growth rate with the longer plasma pulse time. The inset shows the film thickness vs number of PEALD cycles for the sample at 200 °C.

$nm^{-2}cycle^{-1}$), the growth rates were similar. Other characteristics of the 25 °C growth were a 10% lower film density (~2.7 g/cm^3 compared with 3.0 g/cm^3) and higher O to Al ratio (2.1 compared with 1.6) compared to the 200 °C growth. The molar mass for films deposited at 25 °C and 200 °C would be defined by the formula weight of the films. At 25 °C the $Al_2O_{4.2}$ formula mass is 15.2% larger than that of $Al_2O_{3.2}$ at 200 °C. Consequently, this analysis suggests a growth rate of 1.5 Å/cycle at 200 °C and a growth rate of ~1.4 Å/cycle at 25 °C, which are consistent with the measured results. Consequently, the higher O to Al atomic ratio and lower thin film density compensate for the lower value of Al atoms deposited per cycle and similar growth rates are obtained at both 25 and 200 °C.

Given the complicated relationship between the deposition parameters and the growth window, it is difficult to compare growth rates across studies. For example, for PEALD using DMAI, one study reported a growth rate of ~0.9 Å/cycle within 25–400 °C,[21] while another reported 1.2 Å/cycle within 160–250 °C.[32] Both vary from the results reported in this study. These differences in growth rate may be due to the different plasma power, plasma time, flow rate, chamber pressure, equipment setup, all of which may affect the concentration of active oxygen plasma species and thus the growth rate, or the different bubbler temperature. It is evident that a more systematic approach needs to be taken. Unfortunately, these factors are often overlooked, and thus, such disparities in growth rate and window are not uncommon. Even for the well-established TMA-H_2O process, reported values for the growth rate at some temperatures can fluctuate up to 0.5 Å/cycle.[23]

B. Spectroscopic measurement of thin film properties

Since the atomic ratios and the film densities were dependent on temperature even within the growth window, it was reasonable to suggest that other film properties may also be dependent on the deposition conditions. Thus, additional characterization techniques were used to determine the film properties of Al_2O_3 deposited within the growth window. More specifically, XPS was used to determine film composition and chemical states, ELS to determine the band gap, UPS to determine the electron affinity, and SE to determine the index of refraction. The goal of these measurements was to obtain a better understanding of the relation between deposition parameters and film properties, and ultimately enable tuning of desired film characteristics.

Film composition and impurity concentrations were determined by XPS on three different samples. Figure 7 shows the respective XPS survey scan (a), and core level peaks for C 1s (b), Al 2p (c), and O 1s (d) of (i) an as-grown 10 nm Al_2O_3 film deposited at 200 °C and (ii) after 600 °C annealing, and an as-grown 10 nm Al_2O_3 film deposited at 25 °C with (iii) 8s and (iv) 40s O_2 plasma exposure durations. In the survey scan, only Al and O signals were evident with the carbon contamination at or below the XPS detection limit. A low C impurity density was indicated for the 200 °C PEALD Al_2O_3 growth process as shown in Fig. 7(b). However, sample (iii) had a weak C peak, which was ascribed to carboxide groups. Compared with sample (iv), the longer oxygen plasma process led to a reduction of the C

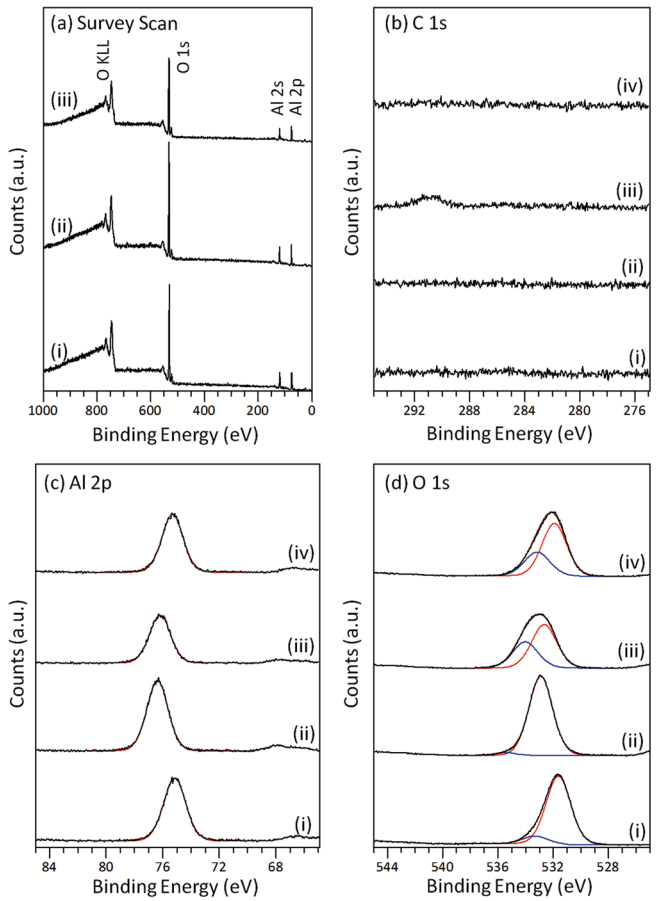

FIG. 7. (Color online) Respective XPS survey scans (a), and core level peaks for C 1s (b), Al 2p (c), and O 1s (d) of (i) an as-grown 10 nm Al_2O_3 film deposited at 200 °C and (ii) after 600 °C annealing, and as-grown 10 nm Al_2O_3 films deposited at 25 °C with (iii) 8s and (iv) 40s O_2 plasma exposure durations.

TABLE I. XPS Al 2p and O 1s core level of Al_2O_3 films deposited at 200 °C and 25 °C before and after annealing. The main core levels and shoulder peaks are differentiated with the full width at half maximum (FWHM) included. All energies given in eV.

		As-grown Al_2O_3				Annealed Al_2O_3			
Growth temperature		Main	FWHM	Shoulder	FWHM	Main	FWHM	Shoulder	FWHM
200 °C	Al 2p	75.2	1.8	-	-	76.4	1.8	-	-
(8 s O_2 plasma)	O 1s	531.6	2.1	533.3	2.2	532.9	2.0	535.4	1.7
25 °C	Al 2p	76.2	1.8	-	-				
(8 s O_2 plasma)	O 1s	532.7	2.1	534.0	2.1				
25 °C	Al 2p	75.3	1.8	-	-	76.6	1.8	-	-
(40 s O_2 plasma)	O 1s	531.9	2.1	533.2	2.2	533.2	2.1	535.7	1.9

peak. Therefore, the conditions of the oxygen plasma can be tuned to improve the film quality and reduce the C impurity density.

Through fitting the peaks with Gaussian–Lorentzian curves, the spectral composition and positions of the Al 2p and O 1s peaks were determined and summarized in Table I. All the samples were characterized by a single Al-O bonding state. This result differs from other results of PEALD Al_2O_3 using DMAI,[21] in which $Al(OH)_3$, AlO(OH), and $Al(CO_x)_y$ configurations were detected for room temperature Al_2O_3, but agrees with another study of room temperature ECR-PEALD Al_2O_3 using TMA.[39] The difference in the bonding states and impurities was likely a result of the different plasma conditions.

On the other hand, the O 1s peaks showed evidence of multiple oxygen bonding states with a distinct shoulder peak at higher binding energy. This peak was likely due to excess oxygen in the film, probably –OH groups. For the 25 °C Al_2O_3 film, the O 1s peak was much broader than that of the 200 °C Al_2O_3 film, which indicated an enhanced oxygen concentration. There may also be a small amount of carbon-based oxide groups, which could be reduced by the longer oxygen plasma process. The increased oxygen concentration was evident in the O to Al atomic ratio, which varied from ~2.1 to 1.9 for the 8 and 40 s O_2 plasma processed 25 °C Al_2O_3 films. This is to be compared with ~1.6 for the 200 °C Al_2O_3 film. It has been suggested that the −OH groups may not be readily removed at lower temperatures,[21] which potentially accounts for the increased oxygen concentration.

The Al 2p and O 1s peak positions were not the same for all the samples. However, the binding energy difference between these two peaks was always 456.5±0.1 eV, which indicated the shifts were caused by different band bending in the SiO_2/Si layers. A previous study has suggested the oxygen plasma process could introduce acceptorlike defects, which may lead to electron transfer from the Si substrate and the formation of an electric field across the SiO_2 layer.[40,41] In this study, the core level of the 200 °C Al_2O_3 film shifted to higher binding energy by ~1.2 eV after 600 °C annealing, suggesting these states could be removed with the annealing process. In the mean time, the relative intensity of the excess oxygen peak decreased from ~10% to 3% after annealing, indicating these acceptorlike states may be related to excess oxygen.[40] For the 25 °C Al_2O_3 film, the shorter oxygen plasma exposure time may induce fewer acceptorlike defects, which apparently resulted in reduced shifts.

Additional characterization was completed for Al_2O_3 deposited on Si at 25 °C and 200 °C as summarized in Table II. ELS was used to determine the band gap. Since ALD Al_2O_3 is amorphous,[31,42] the band gap is typically significantly smaller than that of crystalline sapphire (~8.8 eV) and has been shown to be dependent on the growth method.[43,44] In this study, the O 1s ELS was used to deduce the band gap of Al_2O_3 as shown in Fig. 8. The O 1s ELS measurement was

TABLE II. Al_2O_3 film properties on Si substrates grown by remote PEALD and DMAI at 25 °C and 200 °C.

PEALD	25 °C	200 °C
Growth per cycle	1.5 Å/cycle	1.5 Å/cycle
Al atoms per cycle	3.9±0.3 at.nm^{-2}cycle^{-1}	5.3±0.3 at.nm^{-2}cycle^{-1}
Mass density	2.69±0.04 g/cm^3	2.96±0.02 g/cm^3
[O/[Al ratio	2.1±0.1	1.6±0.1
Refractive index (630 nm)	1.61±0.01	1.63±0.02
Band gap	6.9±0.1 eV	6.7±0.1 eV
Electron affinity	-	2.2±0.1 eV

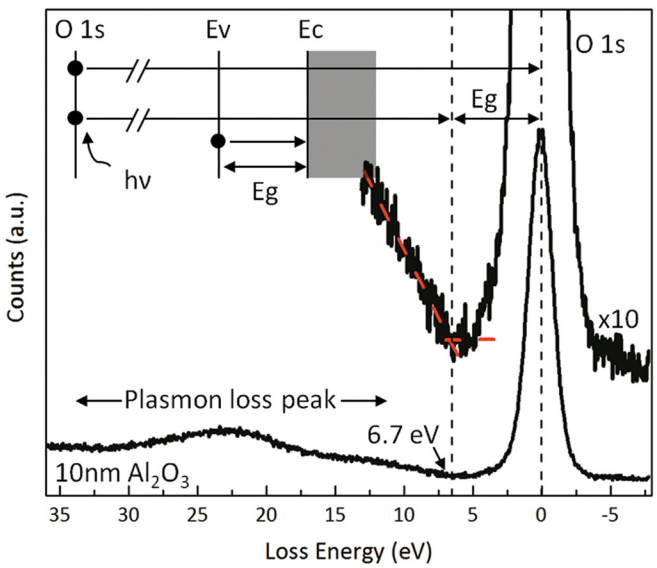

FIG. 8. (Color online) O 1s energy loss spectra from 10 nm Al_2O_3 on Si deposited at 200 °C and annealed at 600 °C. The zero loss energy represents the O 1s core level. Ev is the valence band maximum; Ec is the conduction band minimum; and Eg is the band gap (Ref. 46).

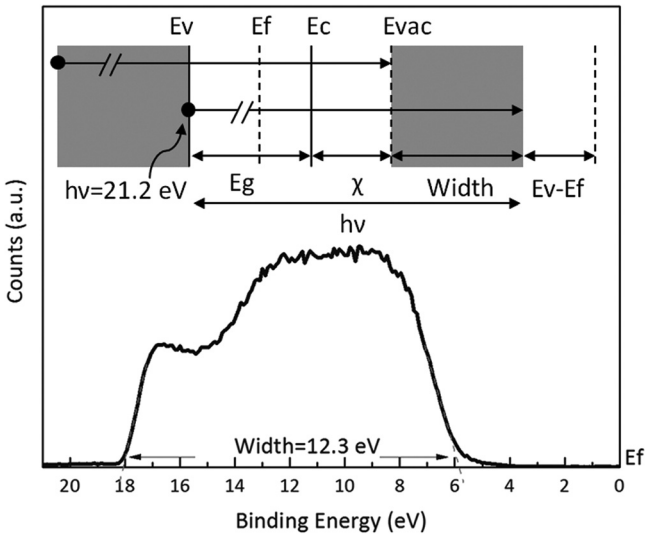

FIG. 9. UPS scan of 1.5 nm Al_2O_3 on Si deposited at 200 °C and annealed at 600 °C. The zero binding energy represents the Fermi level, and the low energy cutoff is the valence band maximum. Ef is the Fermi level; Evac is the vacuum level; and χ is the electron affinity.

obtained from a 10 nm Al_2O_3 film deposited on Si at 200 °C and annealed at 600 °C. A fraction of the emitted O 1s photoelectrons suffer energy loss due to collective oscillations (plasmons) and single particle excitations (band to band transitions).[45,46] The plasmon loss showed a smooth and broad spectral component related to the O 1s core level but shifted to higher binding energy by the plasmon energy. Aligning the O 1s peak to the point of zero energy loss, the onset energy of electron excitations from valence band to conduction band indicated the energy band gap of the films. The band gap was thus determined to be 6.7±0.1 eV. For the annealed, room temperature Al_2O_3 with 40 s O_2 plasma process, the band gap was 6.9±0.1 eV. These values are comparable to other results (6.5–7.0 eV).[6,46,47]

The band gap value could then be used in conjunction with UPS to determine the electron affinity. The UPS spectrum of 1.5 nm annealed Al_2O_3 on Si deposited at 200 °C shown in Fig. 9 is similar to that reported for γ-Al_2O_3 films.[48] The high and low binding energy cutoff could be determined by an extrapolation of a linear fit to the UPS spectrum. The photo threshold energy or ionization energy of VBM electrons was calculated to be 8.9 eV for Al_2O_3 films, which was determined from the energy difference between the photon energy (He I = 21.2 eV) and the UPS spectral width (12.3 eV). This is also the sum of the band gap and electron affinity, as shown schematically in Fig. 9. Using the measured band gap of Al_2O_3, the electron affinity of Al_2O_3 grown at 200 °C was determined to be 2.2±0.1 eV, which is similar to other reports.[6,49]

Additionally, the optical properties of the films were determined by SE, where the index of refraction was 1.63±0.02 for films deposited at 200 °C and 1.61±0.01 for films deposited at 25 °C, which was also consistent with reported results (1.62±0.02) for PEALD-DMAI Al_2O_3.[21] This slight increase with temperature also followed a trend for thermal ALD growth of Al_2O_3 (using TMA).[50] In that case, the index of refraction increased slightly with growth temperature (from 1.57 to 1.60), and a corresponding increase of the film density from 2.7 to 3.0 g/cm^3 was also observed.

IV. CONCLUSION

In this study, Al_2O_3 films were grown on Si by remote PEALD using O_2 plasma and DMAI as an alternative to pyrophoric TMA. The growth parameters—including the DMAI pulse time, O_2 plasma exposure time, N_2 purge time, O_2 plasma power, and substrate temperature—were varied to achieve self-limiting saturated growth, giving a growth rate of ~1.5 Å/cycle within the growth window of 25 °C–220 °C. The growth rate increased with an increase of plasma exposure time and power until the reaction was saturated. This increase was attributed to an increased concentration of active oxygen species on the surface. For deposition at room temperature, a longer plasma pulse time was required to achieve saturated growth. Furthermore, the room temperature deposited Al_2O_3 film with a longer O_2 plasma process displayed a single Al-O bonding state and carbon contamination below the XPS detection limit. Within these optimized growth parameters, conformal, uniform, and nearly stoichiometric Al_2O_3 films were obtained at 200 °C with a film density of ~2.96±0.02 g/cm^3, an index of refraction of 1.63±0.2, and a band gap of 6.7±0.1 eV. Conformal and uniform Al_2O_3 films were also obtained at room temperature with a higher O:Al ratio of 2.1, a film density of ~2.69±0.04 g/cm^3, and an index of refraction of 1.61±0.1. The PEALD-DMAI process, with the significant advantage of a nonpyrophoric precursor, is comparable to PEALD-TMA in both process parameters and film properties.

ACKNOWLEDGMENTS

This research was supported by the Office of Naval Research through the DEFINE MURI program, N00014-10-1-0937, and the National Science Foundation, DMR-1206935. The authors appreciate helpful discussions with Chiyu Zhu, Xin Liu, Tianyin Sun, and Xingye Wang. The authors are also thankful for Emmanuel Soignard, Diana Convey, and Barry Wilkens providing x-ray reflectivity, spectroscopic ellipsometry, and Rutherford backscattering spectrometry measurements through the Leroy Eyring Center for Solid-State Science, respectively.

[1]M. D. Groner, J. W. Elam, F. H. Fabreguette, and S. M. George, Thin Solid Films **413**, 186 (2002).
[2]M. M. Frank, G. D. Wilk, D. Starodub, T. Gustafsson, E. Garfunkel, Y. J. Chabal, J. Grazul, and D. A. Muller, Appl. Phys. Lett. **86**, 152904 (2005).
[3]J. Yang, B. S. Eller, C. Zhu, C. England, and R. J. Nemanich, J. Appl. Phys. **112**, 053710 (2012).
[4]P. D. Ye, B. Yang, K. K. Ng, J. Bude, G. D. Wilk, S. Halder, and J. C. M. Hwang, Appl. Phys. Lett. **86**, 063501 (2005).
[5]B. S. Eller, J. Yang, and R. J. Nemanich, J. Vac. Sci. Technol. A **31**, 050807 (2013).
[6]E. Bersch, S. Rangan, R. A. Bartynski, E. Garfunkel, and E. Vescovo, Phys. Rev. B **78**, 085114 (2008).
[7]N. V. Nguyen *et al.*, J. Vac. Sci. Technol. A **23**, 1706 (2005)
[8]K.-S. An, W. Cho, K. Sung, S. S. Lee, and Y. Kim, Bull. Korean Chem. Soc. **24**, 1659 (2003).
[9]R. Matero, M. Ritala, M. Leskelä, T. Salo, J. Aromaa, and O. Forsén, J. Phys. IV France **9**, 493 (1999).

[10]A. I. Abdulagatov, Y. Yan, J. R. Cooper, Y. Zhang, Z. M. Gibbs, A. S. Cavanagh, R. G. Yang, Y. C. Lee, and S. M. George, Appl. Mater. Interfaces **3**, 4593 (2011)
[11]P. Poodt, A. Lankhorst, F. Roozeboom, K. Spee, D. Maas, and Ad Vermeer, Adv. Mater. **22,** 3564 (2010).
[12]C. Prasittichai and J. T. Hupp, J. Phys. Chem. Lett. **1,** 1611 (2010).
[13]M. D. Groner, S. M. George, R. S. McLean, and P. F. Carcia, Appl. Phys. Lett. **88**, 051907 (2006).
[14]Y. Matsuura and J. Harrington, J. Opt. Soc. Am. A **14**, 1255 (1997).
[15]R. Thielsch A. Gatto, J. Heber, and N. Kaiser, Thin Solid Films **410**, 86 (2002).
[16]P. F. Carcia, R. S. McLean, M. H. Reilly, M. D. Groner, and S. M. George, Appl. Phys. Lett. **89**, 031915 (2006).
[17]T. Maruyama and S. Arai, Appl. Phys. Lett. **60**, 322 (1992).
[18]R. L. Puurunen, J. Appl. Phys. **97**, 121301 (2005).
[19]H. B. Profijt, S. E. Potts, M. C. M. van de Sanden, and W. M. M. Kessels, J. Vac. Sci. Technol. A **29**, 050801 (2011).
[20]B. Lee, S.-Y. Park, H.-C. Kim, K. Cho, E. M. Vogel, M. J. Kim, R. M. Wallace, and J. Kim, Appl. Phys. Lett. **92**, 203102 (2008).
[21]S. E. Potts, G. Dingemans, C. Lachaud, and W. M. M. Kessels, J. Vac. Sci. Technol. A **30**, 021505 (2012).
[22]J. L. van Hemmen, S. B. S. Heil, J. H. Klootwijk, F. Roozeboom, C. J. Hodson, M. C. M. van de Sanden, and W. M. M. Kessels, J. Electrochem. Soc. **154**, G165 (2007)
[23]E. Langereis, J. Keijmel, M. C. M. van de Sanden, and W. M. M. Kessels, Appl. Phys. Lett. **92**, 231904 (2008).
[24]S. E. Potts, W. Keuning, E. Langereis, G. Dingemans, M. C. M. vande Sanden, and W. M. M. Kessels, J. Electrochem. Soc. **157**, P66 (2010).
[25]S. E. Potts, H. B. Profijt, R. Roelofs, and W. M. M. Kessels, Chem. Vap. Deposition **19,** 125 (2013).
[26]J. W. Lim and S. Yun, Electrochem. Solid-State Lett. **7**, F45 (2004).
[27]A. J. M. Mackus, N. Leick, L. Baker, and W. M. M. Kessels, Chem. Mater. **24**, 1752 (2012).
[28]S. J. Lim, S. J. Kwon, H. Kim, and J. S. Park, Appl. Phys. Lett. **91**, 183517 (2007).
[29]E. Langereis, M. Creatore, S. B. S. Heil, M. C. M. van de Sanden, and W. M. M. Kessels, Appl. Phys. Lett. **89**, 081915 (2006).
[30]T. O. Kääriäinen and D. C. Cameron, Plasma Process. Polym. **6**, S237 (2009).
[31]J. G. Lee, H. G. Kim, and S. S. Kim, Thin Solid Films **534**, 515 (2013).
[32]J. Koo, S. Kim, S. Jeon, H. Jeon, Y. Kim, and Y. Wen, J. Korean Phys. Soc. **48**, 131 (2006).
[33]F. Tang, C. Zhu, D. J. Smith, and R. J. Nemanich, J. Vac. Sci. Technol. A **30**, 01A147 (2012).
[34]C. Zhu, S. L. Caudle, J. Yang, D. J. Smith, and R. J. Nemanich, J. Vac. Sci. Technol. B **32**, 011203 (2014).
[35]W. Cho, K. Sung, K.-S. An, S. S. Lee, T.-K. Chung, and Y. Kim, J. Vac. Sci. Technol. A **21**, 1366 (2003).
[36]S. B. S. Heil, P. Kudlacek, E. Langereis, R. Engeln, M. C. M. van de Sanden, and W. M. M. Kessels, Appl. Phys. Lett. **89**, 131505 (2006).
[37]M. Ritala, M. Leskelä, L. Niinistö, and P. Haussalo, Chem. Mater. **5**, 1174 (1993).
[38]S. Y. Lee, B. Luo, Y. Sun, J. M. White, and Y. Kim, Appl. Surf. Sci. **222**, 234 (2004).
[39]Y. Xiong, L. Sang, Q. Chen, L. Yang, Z. Wang, and Z. Liu, Plasma Sci. Technol. **15**, 52 (2013).
[40]C. C. Fulton, T. E. Cook, G. Lucovsky, and R. J. Nemanich, J. Appl. Phys. **96**, 2665 (2004).
[41]C. Zhu, D. J. Smith, and R. J. Nemanich, J. Vac. Sci. Technol. B **30**, 051807 (2012).
[42]M. L. Huang, Y. C. Chang, C. H. Chang, Y. J. Lee, P. Chang, J. Kwo, T. B. Wu, and M. Hong, Appl. Phys. Lett. **87**, 252104 (2005).
[43]I. Costina and R. Franchy, Appl. Phys. Lett. **78**, 4139 (2001).
[44]R. H. French, J. Am. Ceram. Soc. **73**, 477 (1990).
[45]F. G. Bell and L. Ley, Phys. Rev. B **37**, 8383 (1988).
[46]H. Nohira *et al.*, J. Non-Cryst. Solids **303**, 83 (2002).
[47]H. Y. Yu *et al.*, Appl. Phys. Lett. **81**, 376 (2002).
[48]A. Jimenez-Gonzalez and D. Schmeisser, Surf. Sci. **250**, 59 (1991)
[49]S. Miyazaki, J. Vac. Sci. Technol. B **19**, 2212 (2001).
[50]M. D. Groner, F. H. Fabreguette, J. W. Elam, and S. M. George, Chem. Mater. **16**, 639 (2004).